Contents lists available at ScienceDirect

Journal of Non-Crystalline Solids: X

Impact of solution pH (5–9) and dissolution products on *in vitro* behaviour of the bioactive glass S53P4

Minna Siekkinen, Markus Engblom, Leena Hupa [*]

Johan Gadolin Process Chemistry Centre, Åbo Akademi University, Henrikinkatu 2, Turku 20500, Finland

ARTICLE INFO

ABSTRACT

The impact of dissolution products on the reaction behaviour of bioactive glasses was explored. Bioactive glass S53P4 particles were immersed in solutions with initial pH of 5–9. After 24 and 72 h, the solution extracts were used for testing unreacted particles. The pH, ion concentrations, and glass surfaces were analysed as functions of immersion time. More Ca, Na, and P dissolved at lower pH (5) than at higher pH (7.4 or 9). The dissolution changed from an incongruent to an apparent congruent with increasing pH. Dissolution products in extracts changed the reaction layer structure on glass particles and led to lower ion release at pH 7.4 and 9. Dissolution increased almost linearly with time in acidic solutions. Silica-rich layer and calcium phosphate were identified on the particles after immersion in all solutions except at pH 9. Local ion concentration variations affected dissolution, leading to nonuniform ion release rates.

1. Introduction

Bioactive glasses are commonly characterised by their ability to form a chemical bond with living tissues, mainly bone, through the hydroxyapatite layer that develops at the glass surface *in vivo* [1]. Controlled degradation and release of ions are unique properties of bioactive glasses [2]. Since their discovery in the late 1960s [3], bioactive glasses have evolved from bone grafting materials to implants and scaffolds for various tissue engineering applications [4–6]. Professor Hench, the inventor of bioactive glasses, observed the strong bond between bone and silicate-based glasses of a narrow composition range. The first bioactive glass reported by Hench is known as Bioglass® 45S5 [7]. The oxide composition of this glass is (in wt%) 45 SiO_2, 24.5 CaO, 24.5 Na_2O, and 6 P_2O_5 [8].

Today, a wide range of glass compositions has been studied for their potential bioactivity. For example, bioactive glass S53P4 with higher silica and lower contents of the other oxides compared to 45S5 showed desired properties for bone tissue applications in several *in vitro, in vivo* and clinical studies [9]. Today, 45S5 and S53P4 are widely used in commercial implant products in the human body [9–13]. Besides stimulating bone growth, S53P4 showed antibacterial effects *in vitro* against 29 aerobic and 17 anaerobic bacteria [14,15]. Clinical studies verified its suitability for treating osteomyelitis in long bones [16,17]. The antibacterial properties are suggested due to the dissolution behaviour of bioactive glasses [18], *i.e.*, the increased pH and the increased ion concentrations in the surrounding solution. Additionally, the release of ions from the glass was verified to stimulate cellular processes in bone regeneration and, accordingly, to produce new bones in an injured site [19].

Similar reactions between the bioactive glass and surrounding solution occur *in vivo* and *in vitro*. The reactions are rapid and are proposed to take place in the following five steps [20]: [i] ion exchange of the alkali and alkaline ions in the bioactive glass surface with the hydrogen ions in the solution, [ii] increase of the solution pH, followed by the release of soluble silicon groups ($Si(OH)_4$) from the glass, [iii] condensation and repolymerisation of silicon on the glass surface to a silica-rich layer, [iv] migration of Ca^{2+} and PO_4^{3-} groups from the glass and precipitation from the solution to amorphous calcium phosphate (Ca/P) layer, [v] crystallisation of the Ca/P-layer to a hydroxyapatite layer as a result of carbonates and hydroxyls incorporating from the surrounding solution. *In vivo* mechanisms then conclude the bonding to the bone.

The dissolution rate of bioactive glasses depends, among other things, on the solution pH, glass surface area to solution volume ratio, and solution composition [21]. An early study showed that the extraction of alkali ions from a binary alkali silicate glass (K_2O-SiO_2) decreased rapidly above pH 9 [22]. Also, calcium dissolved more rapidly from bioactive glass 45S5 in an acidic solution (pH 5) compared to neutral (pH 7.4) and alkaline (pH 9) solutions [23]. On the other hand, at
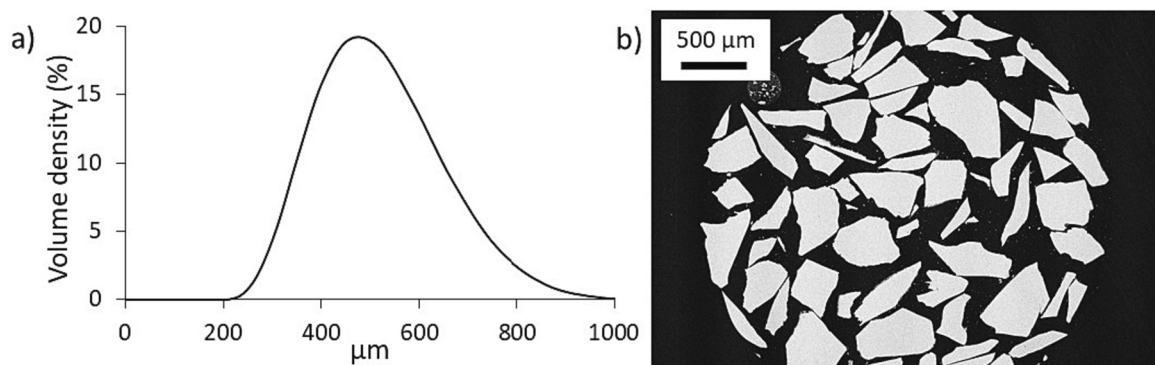

Fig. 1. Particle size distribution (a) and cross-sectional SEM image (b) of unreacted S53P4 particles.

increased pH levels, Si is expected to dissolve more rapidly than alkalis. The critical pH level of increased Si dissolution from the glass structure is pH 9 [24]. As smaller particles have a larger surface area, they dissolve faster than larger particles [25]. In addition, particles in a cascade reactor, *i.e.*, in separate reactors connected in series, were reported to react differently in a continuous solution flow due to increasing concentration of dissolution products [26]. This implies that particles inside an implanted bioactive glass particle bed will be in contact with a solution already containing dissolution products from the outer bed particles. Consequently, these interior particles likely experience a higher pH than the outer particles. However, the dynamic body system strives to maintain the pH of the extracellular fluid constant, *i.e.*, around 7.4 [27]. At the same time, the pH can be within 5.5–6.7 at bone infection sites [28]. Even lower local pH levels can occur if the bioactive glass is used as a component in a composite with a biodegradable polymer, *e.g.*, polylactic acid, giving an acidic environment due to degradation reactions [29]. Also, the oral cavity can experience an environment with decreased pH due to the intake of drinks or food with a lower pH [30]. On the other hand, locally increased pH at the implant site can appear at the glass/solution interface and affect the dissolution behaviour of the glass [31].

Immersing bioactive glass in a static solution is a standard procedure when investigating *in vitro* behaviour [32]. Experiments conducted with solutions containing dissolution products from bioactive glasses are limited and mainly focused on the biological response. For example, the human osteoblast growth cycle was shortened when ions dissolved from bioactive glass 45S5 were present [33]. Furthermore, ions dissolving from bioactive glasses induced osteogenesis *in vitro* [34]. Dissolved ions from an experimental bioactive glass promoted strong mineralization of human adipose stem cells in hydrogels [35]. Similarly, ions common in bioactive glasses have been identified to induce HA precipitation (aqueous Si) [36], increase osteoblast proliferation and differentiation, increase mineralization of the extracellular matrix (Ca ions) [37], and stimulate the main protein (matrix Gla protein) for bone formation (phosphate) [38]. In a dynamic environment, the increase of ion concentrations and, consequently, the decrease of available hydrogen ions for ion exchange have been proposed to delay the reactions of bioactive glasses [26,39]. However, the impact of dissolution products in the solution on the reaction behaviour of bioactive glasses at different pH levels is not fully understood.

This study aimed to investigate bioactive glass S53P4 particles in different environments that could occur in the human body, including changes in the surrounding solution pH due to infection or material/solution reactions. Also, the solution composition might change as it flows in voids of particle beds or porous bodies, thus affecting the reactions in various parts of the implanted material. In this work, the reactions of bioactive glass S53P4 particles were studied in solutions at three pH levels (5–9) in static conditions for up to 120 h. In addition, the extracts after 24 and 72 h of dissolution were reused to study the impact

of increased ion concentrations on the dissolution of unreacted particles. The results give indications of the dissolution mechanisms of bioactive glasses in various *in vitro* and *in vivo* conditions.

2. Materials and methods

2.1. Bioactive glass samples

Bioactive glass S53P4 (in wt%) 53 SiO_2, 20 CaO, 23 Na_2O, and 4 P_2O_5 was produced by mixing quartz sand with analytical grade reagents Na_2CO_3, $CaHPO_4 \cdot 2H_2O$, and CaO_3. The batch was added into a platinum crucible and melted in an electric furnace at 1360 °C for 3 h. The melt was cast in a graphite mould to give a glass bar, annealed at 520 °C for 1 h and cooled down to room temperature in the oven. The bar was crushed and remelted to obtain a homogeneous glass. Finally, bioactive glass particles were produced with a ring and puck mill. Particles that passed through a 500 μm sieve but stayed on a 300 μm sieve were used for the immersion studies. Before immersion, the particles were cleaned in acetone in an ultrasound bath to remove fine powder adhered to the particle surfaces. Fine, rapidly dissolving powder might affect the accuracy of dissolution studies [40]. Fig. 1 shows a) the particle size distribution (Malvern Panalytical Mastersized 3000) and b) an SEM image of the S53P4 particle cross-sections. The median diameter of the analysed particles was 445 μm, and 69% were in the size range of 310–516 μm. 28% of the particles were > 516 μm, and 3% were < 310 μm. The irregular-sized particles increased the possibility of elongated particles passing through the sieve, contributing to the increased particle size distribution.

2.2. Immersion solutions

Tris(hydroxymethyl)aminomethane (Tris), with the pH indicated in parenthesis after the solution symbol, was prepared using the reagents given in Table 1. The pH of Tris (5) was adjusted using acetic acid instead of the usual hydrochloric acid (HCl) to minimize the risk of Cl ions interfering with the apatite formation on the glass particle surfaces

Table 1

Reagents for 0.5 l buffer solutions, solution pH, and calculated base and acid molarities of the solutions at 37 °C.

	Tris (g)	HAc (ml)	HCl (ml)	NaOH (ml)	pH	base (mM)	acid (mM)
Tris (9)	**3.03**	–	1.5	–	9	50	3
Tris (7.4)	**3.03**	–	17.9	–	7.4	50	36
Tris (5)	**3.03**	24.7	–	–	5	50	50
HAc (5)	–	**3**	–	34.1	5	68	100

Table 2
pH as functions of the immersion time for the solutions used to dissolve S53P4 particles: as-prepared (0), extracted after 24 h (24) and 72 h (72). Bold values indicate the pH measured above the glass particles at 24 and 72 h, while the underlined values give the extracted and mixed solution pH before adding new particles.

h	Tris 9			Tris 7.4			Tris 5			HAc 5		
	(0)	(24)	(72)	(0)	(24)	(72)	(0)	(24)	(72)	(0)	(24)	(72)
0	8.97	9.12	9.10	7.35	7.46	7.58	4.96	5.09	5.15	4.93	5.05	5.08
2	9.10	9.15	9.11	7.44	7.57	7.59	5.06	5.11	5.19	5.01	5.05	5.11
4	9.11	9.15	9.12	7.46	7.53	7.61	5.07	5.12	5.22	5.05	5.07	5.14
6	9.12	9.15	9.14	7.47	7.52	7.62	5.08	5.13	5.24	5.03	5.09	5.16
8	9.13	9.17	9.15	7.49	7.53	7.59	5.10	5.15	5.26	5.04	5.08	5.17
24	**9.15**	9.20	9.17	**7.52**	7.57	7.69	**5.15**	5.23	5.32	**5.11**	5.14	5.17
48	9.23	9.25	9.28	7.59	7.60	7.69	5.26	5.26	5.48	5.16	5.15	5.24
72	**9.31**	9.29	9.33	**7.62**	7.64	7.71	**5.26**	5.36	5.55	**5.16**	5.20	5.29
96	9.31	9.34	9.37	7.62	7.65	7.73	5.27	5.35	5.60	5.23	5.25	5.35
120	9.38	9.37	9.41	7.66	7.68	7.75	5.38	5.42	5.68	5.27	5.30	5.40

[41]. The buffer capacity of Tris is between 7 and 9 [42]. Therefore, an additional HAc-NaOH (HAc) buffer solution was used for immersion studies within the buffering range of 3.6–5.6. The reagents (in bold, Table 1) were added to purified water and wholly dissolved before the temperature of the solutions was increased in a water bath to 37 °C. Finally, the pH of the solutions was adjusted by slowly adding 1 M HCl, 1 M HAc, or 1 M NaOH under continuous stirring. The theoretical mass/volume and molarity of the acids and bases are also presented in Table 1. The acid and base concentrations for the desired buffer pH values were calculated using the Henderson-Hasselbalch equation [43], with the pKa (37 °C) of Tris as 7.8 and of HAc as 4.67.

2.3. Immersion tests

A shaking incubator (Stuart Orbital Incubator SI500) with a rotation speed of 100 rpm at 37 °C was used for the immersions. 210 ± 5 mg of bioactive glass particles were added in 30 ± 0.1 ml solution in a covered polypropylene centrifuge tube (50 ml). Assuming spherical particles with an average diameter of 400 μm gave an approximate surface area to volume ratio of 0.4 cm^{-1}. The immersion tests were carried out for 24, 72, and 120 h. The 120 h experiments had three parallel runs. The pH of the solutions was measured every other hour for up to 8 h, and from 1 day forward, every 24 h. At hours 8, 24, and 72, an aliquot of 1 ml was extracted for ion analysis. Further, the ion concentrations were measured at 120 h. The reacted particles were washed with ethanol and dried at 40 °C before being stored in a desiccator until further analyses.

Additional glass samples were immersed for 24 and 72 h to achieve extracts for investigating the effect of the released ions on the dissolution of new, unreacted S53P4 particles. For a surface area to volume ratio similar to the initial immersion tests (0.4 cm^{-1}), 202 ± 3 mg of bioactive glass particles were immersed in 28.5 ml of the extracted solutions. The solutions and glass particles were collected for further analyses at the same measurement points as experiments with as-prepared solutions.

2.4. Change of solution pH

The pH is temperature dependent and was therefore measured by placing the vials with the immersed particles in a 37 °C water bath to keep the temperature constant during the pH measurement. The measurements were conducted close to the particle bed without the pH electrode touching the particles. The pH has been shown to increase the closer the pH electrode is to the particle bed in a container [44]. However, the agitation during the immersion likely contributed to equalising pH throughout the solution. Also, the pH of the reference solutions, kept in the same incubator as the bioactive glass immersion solutions, was measured at 0 and 120 h. The pH-meter (VWR pHenomenal pH 1100 L) was calibrated with the pH standards 4.01 and 7.00 (25 °C).

2.5. Ion analysis

The collected solutions were analysed with inductively coupled plasma-optical emission spectrometry (ICP-OES, Optima 5300 DV; Perkin Elmer, Waltham, MA). The extracted 1 ml solution was diluted with 9 ml of purified water. The ICP was calibrated with 1, 5, and 20 ppm commercial (Spectrascan) multi-element standards of Si, Ca, Na, and P. Before and after the measurements, the background level was recorded by analysing the 1 ppm standard of each element. The reported ion concentrations were background corrected accordingly. The elements were analysed with the limit of quantification (LOQ) Si = 0.04 mg/l, Ca = 0.003 mg/l, Na = 0.2 mg/l, and P = 0.03 mg/l. Ion analysis was conducted for three parallel samples, and each sample was analysed 3–5 times. Aliquots were extracted at 8, 24, and 72 h, so the surface area to volume ratio changed accordingly. Therefore, the measured values were calculated according to Eq. (1) [45].

$$C_{i,j}^* = C_{i,j} + \frac{V^a}{V^s} \sum_j^N C_{i,j-1} \qquad (1)$$

where $C_{i,j}^*$ is the normalised concentration of element i at time j, $C_{i,j}$ the measured concentration of element i at time j, V^a the volume of the extracted aliquot, V^s the volume of the immersion solution before extraction of the aliquot, and $C_{i,j-1}$ the measured concentration of element i at time point $j-1$. The normalised mass loss of each element was then calculated according to Eq. (2) [46].

$$NL_i = \frac{C_i^* - C_0}{\left(\frac{SA}{V}\right)f_i} \qquad (2)$$

where NL_i is the normalised loss of each element (g/m^2), C_i^* is the normalised ion concentrations of element i calculated with Eq. (1) (mg/l), C_0 is the ion concentration of element i measured with ICP-OES in the reference solution (mg/l), SA is the total surface area of the unreacted immersed glass particles (m^2), V is the volume of immersion solution (l), and f_i is the mass fraction of element i in the unreacted glass sample.

2.6. Glass surface analysis

After 120 h, the glass particles from the dissolution experiments in the four as-prepared immersion solutions and their 24 and 72 h extracts were embedded in epoxy resin. The embedded particles were ground and polished with abrasive sandpaper to reveal the cross-sections. A scanning electron microscope (SEM, Leo Gemini; Carl Zeiss, Oberkochen, Germany) was used to take images of the cross-sections and the surfaces of particles immersed for 120 h. For particles with visible layer formations, energy dispersive X-ray line analysis (EDX, Leo Gemini; Carl Zeiss, Oberkochen, Germany, coupled with SEM) of the cross-sections was also taken.
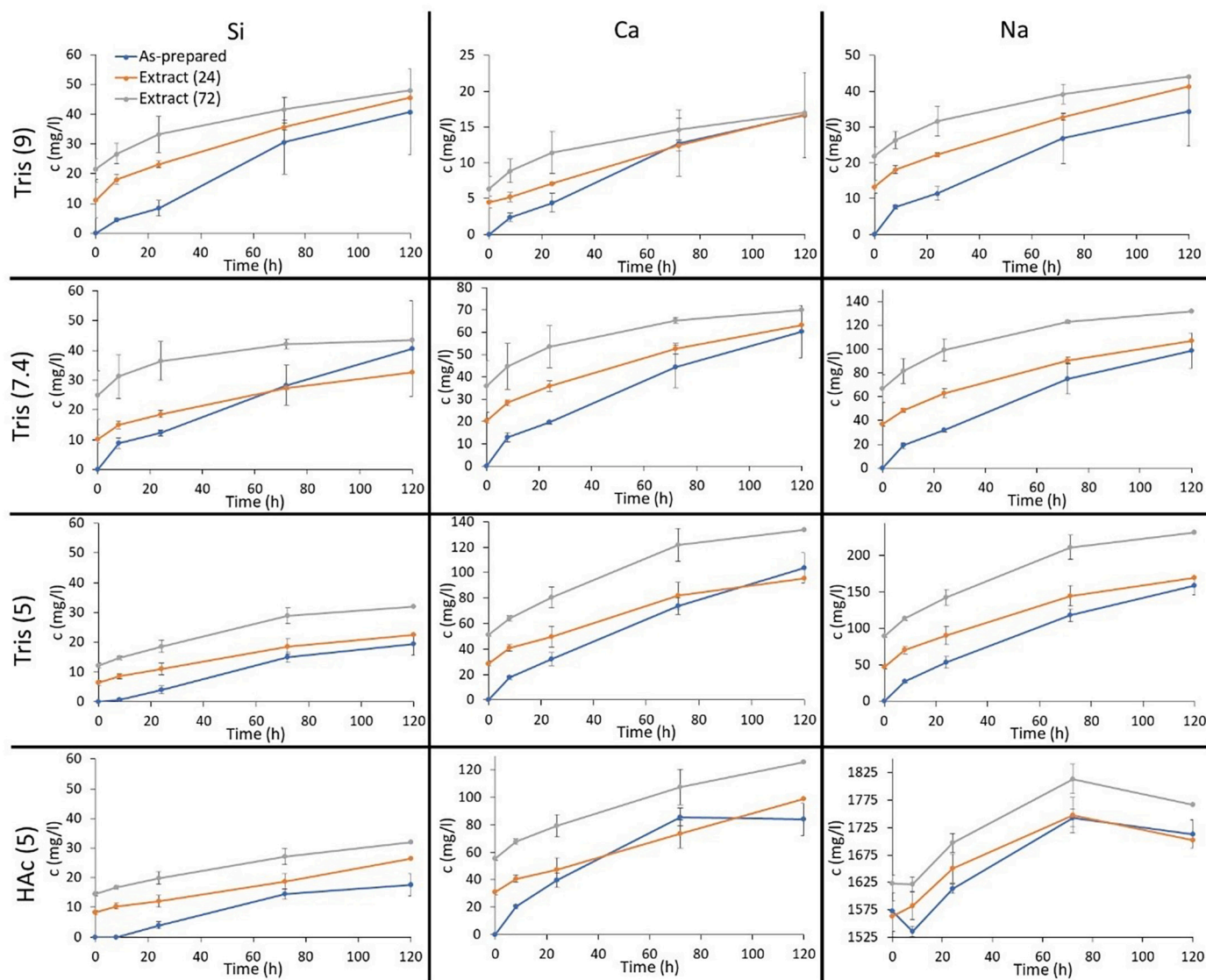
Fig. 2. Normalised ion concentrations of Si, Ca, and Na in the solutions during 120 h dissolution of S53P4 particles.

3. Results

3.1. pH of immersion solutions

Table 2 shows the average pH of the four immersion solutions as functions of the immersion time, where 0 indicates the as-prepared solutions, and 24 and 72 are for the extracts. Due to the minor pH differences between the parallel samples, the table does not include the variations. The three measured parallel samples for the immersion using the as-prepared solutions gave a variation of ±0.04 (Tris 9), ± 0.02 (Tris 7.4), ± 0.02 (Tris 5), and ± 0.02 (HAc 5) pH units. Similarly, the variations in immersions using the extracts were also minor, *i.e.*, ± 0.01 – ± 0.08 pH units. The pH values of the supernatants measured above the glass particles at 24 and 72 h are marked in bold, and the pH of the extracted and mixed solutions before adding new particles are underlined in Table 2. The difference between the two pH values for the supernatant and extract varied between 0.03 and 0.21 pH units depending on the solution. These differences were likely due to the time lag for pH equalisation throughout the solution. However, as the pH of all samples containing glass particles was measured similarly, the pH trends for each solution were assumed to correlate with the progress of the glass reactions. In addition, the total volume of the solutions decreased by up to

3 ml due to the sampling of the aliquots for elemental analysis. Thus, the pH from 24 to 96 h cannot directly be compared with pH values measured at earlier points or 120 h. The pH of all solutions increased with increasing immersion times and was highest for the immersions done using the 72 h extracted solutions.

3.2. Ion analysis

Fig. 2 shows the normalised Si, Ca, and Na concentrations (mg/l) in the static solutions as functions of time. As the pH of HAc (5) was adjusted with NaOH, the high Na levels in the solutions (1570 mg/l in the as-prepared solution) questioned the accuracy of Na in HAc solutions. However, the Na concentration trends in HAc (5) and its extracts were assumed to correlate with the Na release. In general, the ions released from S53P4 particles into the solutions increased with immersion time but in lower concentrations when using the extracts.

Similar Si concentration levels were measured in the as-prepared Tris (9) and Tris (7.4) throughout the immersions. In contrast, the Si concentration was lower in the as-prepared Tris (5) and HAc (5). Interestingly, the Si concentrations increased roughly linearly with time in the as-prepared solutions and extracts of Tris (5) and HAc (5), independent of the concentration before the immersion. However, the changes

Table 3
Concentration of P (mg/l) after the dissolution of S53P4 particles in the as-prepared solutions (0) and extracts (24 and 72). n/a = values below the LOQ.

Time (h)	Tris (9)			Tris (7.4)			Tris (5)			HAc (5)		
	(0)	(24)	(72)	(0)	(24)	(72)	(0)	(24)	(72)	(0)	(24)	(72)
0	n/a	n/a	n/a	n/a	n/a	0.2	n/a	n/a	n/a	n/a	0.3	0.8
8	n/a	n/a	n/a	0.3	n/a	0.7	n/a	0.5	0.5	n/a	0.9	1.4
24	n/a	n/a	n/a	0.5	n/a	0.7	0.1	0.5	0.8	0.7	0.9	1.5
72	n/a	n/a	n/a	0.4	n/a	0.6	0.5	0.7	1.5 ± 1	1.8 ± 1	1.3	1.8
120	n/a	n/a	n/a	0.8 ± 1	n/a	0.5	1.9 ± 1	0.7	1.3	1 ± 1	1.9	2.8

Fig. 3. SEM images of S53P4 particles immersed in the four as-prepared solutions and their 24 and 72 h extracts for 120 h.

in Si concentration during 120 h dissolution in the as-prepared Tris (9) at its 72 h extract were 41 mg/l and 26 mg/l. Corresponding values for the as-prepared Tris (7.4) and its 72 h extract were 41 mg/l and 18 mg/l, respectively.

The lowest Ca and Na concentrations were measured in Tris (9). Ca and Na releases were the least in the 72 h extract of Tris (9). Correspondingly, the highest Ca and Na concentrations were measured in Tris (5) and HAc (5). For most solutions, the concentration of P species was close to or below the limit of quantification (LOQ), as shown in Table 3.

3.3. Glass particle surface changes

Fig. 3 shows SEM images with two magnifications of S53P4 particle cross-sections immersed for 120 h in the four as-prepared solutions and their two extracts. It should be noted that not all particles in the sample had formed similar surface reaction layers, as shown in the figure. The magnified images present typical single particles with distinct changes in the surface composition. Notably, no distinct layers were seen after the dissolution in Tris (9). After the dissolution in all other solutions and extracts, typical silica-rich and calcium phosphate layers were identified on the particle surfaces. The thickness of the silica-rich layer seen with the dark-grey colour increased with the decrease of the solution pH.

Fig. 4 shows SEM images of particle surfaces before and after 120 h in the four as-prepared solutions in two magnifications. Even though the cross-sectional images of Tris (9) immersed particles (Fig. 3) did not show any reaction layers typical for bioactive glasses *in vitro*, the surface images suggest glass corrosion. After the immersion in Tris (7.4), large cracks typical for SEM images of the silica-rich layer are seen in the particle surfaces. The accumulations after the immersions consisted of calcium phosphate (Fig. 5). Similarly, the cracks in particles immersed in Tris (5) and HAc (5) suggest a silica-rich layer. Some calcium phosphate precipitates had also formed in these solutions.

The element composition of the surface layers on the particles after 120 h in all solutions except the Tris (9) is given by the EDX line analyses
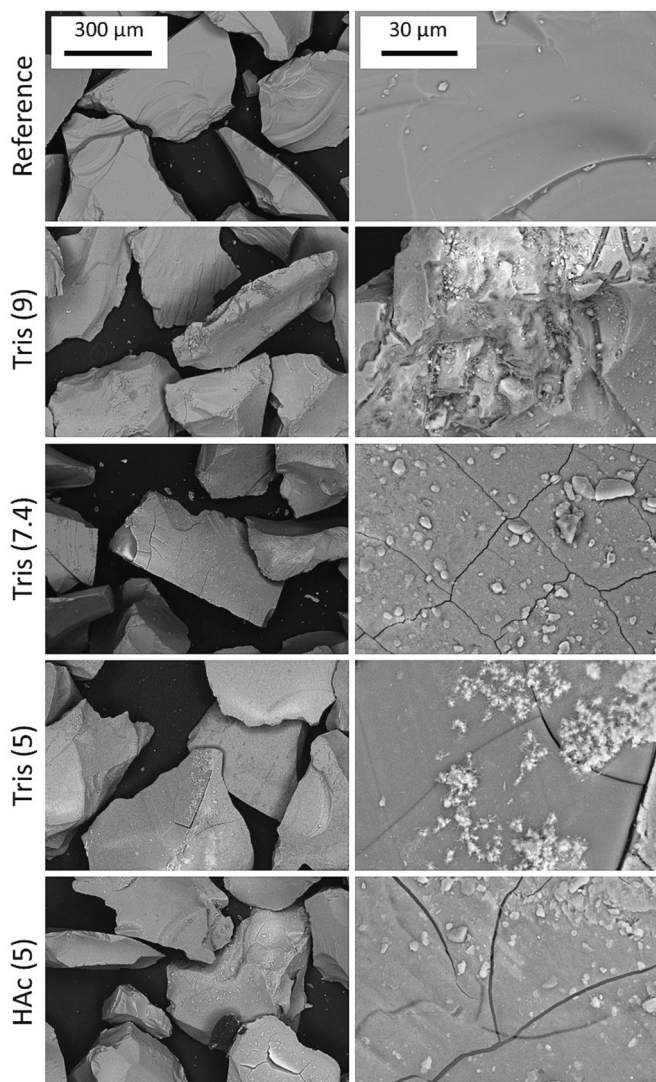
Fig. 4. SEM images of S53P4 particles before (Reference, 0 h) and after immersion (120*h*) in the as-prepared solutions in two magnifications.

in Fig. 5. After the immersion in Tris (7.4), the line analyses indicate a silica-rich layer next to the bulk glass (start of the arrow). The silica-rich layer appears thicker and almost free of Ca, Na, and P for the as-prepared solution. Then, the outermost layer suggests peaks of Ca and P in molar ratios typical for hydroxyapatite. After the immersion in the 24 and 72 h extracts, Ca and P are also present in the silica-rich layer. However, after immersion in Tris (5), the silica-rich layer appears thicker and is almost free of Ca and P.

4. Discussion

Immersion of bioactive glasses in Tris buffer enables a significantly easier comparison of dissolution reactions than studies in the complex simulated body fluid (SBF) [47,48]. In this work, Tris buffer solutions and their extracts after 24 and 72 h immersion of bioactive glass S53P4 were used to gain an increased understanding of the impact of dissolution products in the solution on surface reactions leading to tissue bonding of bioactive glasses. Earlier studies *in vitro* have been conducted with, for example, 75 mg of small particles (<50 μm in diameter, some even 2 μm) immersed in 50 ml of buffered solutions [23,41,49,50]. Such small particles have a large surface area, leading to much faster glass dissolution and, consequently, a notable increase in the pH of the surrounding solution. For example, inside a bed of S53P4 particles of a

diameter of <45 μm, the pH of SBF had increased to 11 after 24 h, while for particles in the size range of 315–500 μm, the pH had increased to 8.6 [51]. Therefore, using larger particles, 300–500 μm, was assumed to retard the rapid initial reactions.

Fig. 6 shows the normalised mass loss rate from the original samples of S53P4 particles in the as-prepared solutions and their extracts for 120 h and the dissolution of elements (mol%) at 120 h. The ion concentrations dissolved in the extracts at 120 h were calculated as the difference between the values at the beginning of the experiment (0 h) and after 120 h (Fig. 2).

In Tris (9) and its extracts, the release of Si, Ca, and Na was around 1 to 3 mol%, suggesting congruent dissolution within the experimental error. The normalised mass loss rate also shows similar dissolution throughout the immersion time. However, the dissolution of alkalis was much less in Tris (9) than in the other solutions, thus explaining that no reaction layers could be verified at the surface (Figs. 3 and 4). This decrease in the dissolution rate aligns with the observations from the dissolution studies of borosilicate glasses, for which the dissolution rate markedly decreased around pH 9 [52]. The phosphorous levels below LOQ (Table 3) also implied a minor dissolution. After 120 h, the pH was slightly higher for the extracts than as-prepared Tris (9). Further, it was assumed that the local solution pH next to the dissolving particles was higher than the measured supernatant pH above the particles [44]. Consequently, network dissolution of the glass above pH 9 led to a slow congruent dissolution of Si, Ca, and Na. On the other hand, the dissolved amount of the glass decreased with increasing content of dissolved ions in the extracts, thus suggesting that the impact of dissolution products retarded the reactions. In a study immersing the International Simple Glass in a Si-saturated solution with a starting pH of 9 at 90 °C, an amorphous alteration layer formed on the glass surface hindered the Si network dissolution [52]. Similarly, Si in the immersion solution hindered the dissolution. In the present work, the maximum initial Si in Tris (9) was 22 mg/l compared to 260 mg/l in the saturated Si study [52]. Interestingly, this small increase in the Si concentration in the solution also slowed the dissolution. However, it should be emphasised that the four-oxide bioactive glass S53P4 contains only one network former compared to two or three in the more complicated aluminoborosilicate glasses studied for an enhanced understanding of the dissolution mechanisms in alkaline solutions [52]. The lack of an alteration layer on the bioactive glass S53P4 implies that the experimental time was too short for a detectable surface layer to form. The low network connectivity might have also supported congruent dissolution at pH 9.

The higher dissolved amounts of Na and Ca than Si in Tris (7.4) suggest incongruent dissolution typical for bioactive glasses (Fig. 6). The higher the concentrations of dissolved ions in the extracts, the less the concentrations increased during the 120 h immersions in Tris (7.4). Interestingly, the accumulation of calcium and phosphate on the glass surface and in the silica-rich layer during the immersion in the extracts suggests that calcium and phosphate ions in the solution affected the diffusion of the released ions through the silica-rich layer (Figs. 4 and 5). The pH of the as-prepared Tris (7.4) and its extracts slightly increased but was well within the buffering range throughout the immersions (Table 2). Na, Ca and P concentration profile changes were sharp at the interface of the unreacted glass and silica-rich layer after the dissolution in the as-prepared Tris (7.4) (Fig. 5). However, the Ca and P profiles were less steep for the particles immersed in the extracts. Thus, the diffusion of the ions through the alteration layer on the glass particles was retarded by the increased ion concentrations in the solution or by early precipitated calcium phosphates on the surface. A further implication is that increasing concentrations of released ions might locally retard the reactions of implants based on bioactive glass S53P4.

Finally, the dissolution of S53P4 particles was highly incongruent in the acidic solutions, Tris (5) and HAc (5) (Fig. 6). The thick silica-rich layers also verify the rapid release of Ca and Na ions (Figs. 3 and 5). Interestingly, the silicon release was almost constant in the as-prepared solutions and their extracts. This implies that the dissolution of the silica
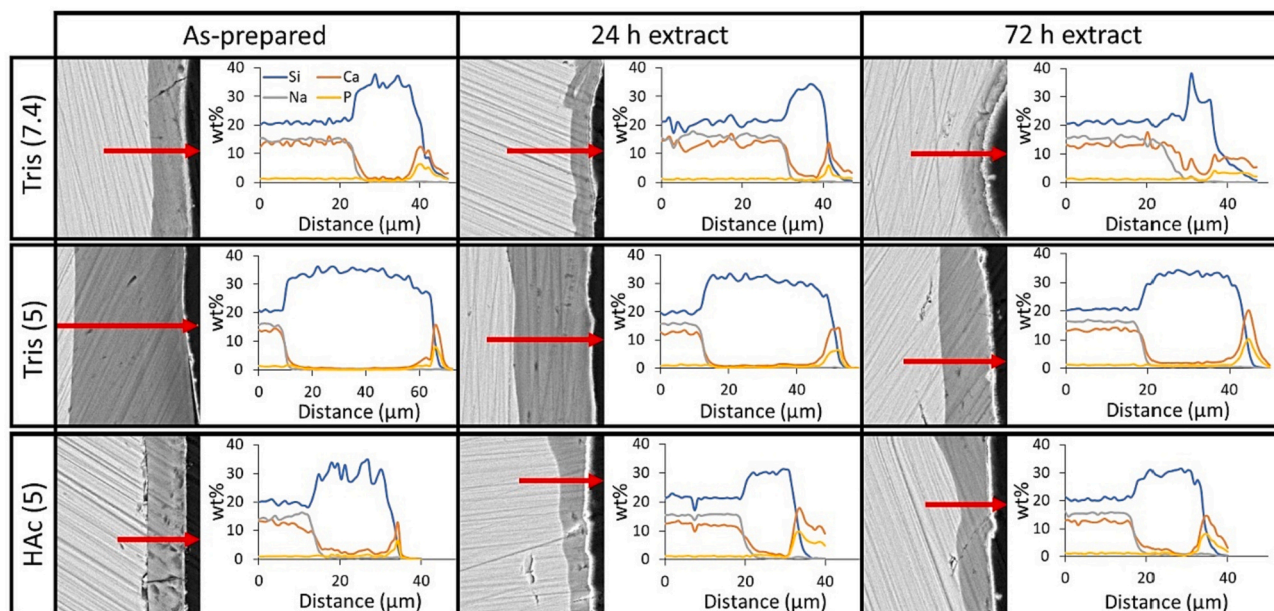
Fig. 5. EDX line analyses of S53P4 particles after 120 h in as-prepared solutions of Tris (7.4), Tris (5) and HAc (5) and their extracts.

network was not affected by the dissolution products in the solution but depended on the immersion time. The pH of the solution increased to 5.2–5.7, thus favouring the precipitation of calcium phosphate species [29]. However, the release trends of Ca and Na ions imply a slight decrease caused by the dissolution products in the solution. No apparent differences were observed in the dissolution of the glass particles in Tris (5) and HAc (5), most likely due to the relatively small differences in the pH of the solutions at different time points. Thus, the reaction mechanisms were similar, and the high content of hydrogen ions in the solutions favoured rapid ion exchange with Ca and Na ions, *i.e.*, incongruent dissolution. The Si release increased with time and likely correlated with the low network connectivity and silica content in S53P4.

Interestingly, the dissolved Si concentrations were almost similar in Tris (9) and Tris (7.4). Tris (7.4) solution was well within the buffering range, while the pH of Tris (9) did not markedly increase beyond the range. This implies that classical hydration and ion exchange reactions can be used to describe the *in vitro* behaviour of silicate-based bioactive glasses. These reactions led to the formation of thick silica-rich layers on the particles in Tris (7.4). Whether this took place through the classical multistep mechanism, including the ion exchange of mobile cations to protons in solution, followed by protonation, condensation and repolymerisation to form a silica-rich layer or through an interfacial-dissolution-re-precipitation mechanism is unclear [53]. In contrast, the dissolution was congruent but markedly slower already at pH 9, with no detectable silica-rich layer. The higher dissolution of Ca and Na ions in Tris (7.4) and its extracts can be explained by the higher concentration of hydrogen ions available for ion exchange between the glass particles and solution. This results in slower ion release at a higher pH [23].

Partly reacted bioactive glasses have been reported to continue dissolving in replenished solutions [54]. This work investigated the reversed situation when extracts with dissolved ions were added to unreacted S53P4 bioactive glass particles. The dissolution reactions were not hindered but retarded by dissolution products in the extracted solutions. The observations imply that the dissolution of, *e.g.*, the outer section of a porous implant exposed to an extracellular solution with the nominal composition will affect the dissolution of the inner sections of a porous implant or particle beds. Ca ions in the solution have been suggested to promote apatite precipitation on bioactive glasses [55]. Dynamic *in vitro* studies of bioactive glasses 45S5 and S53P4 using

solutions buffered at pH 7.4 indicated that the formation of reaction layers was delayed when the concentration of dissolution products in the solution increased [26,39]. The static tests in this work showed that the dissolved ions from the bioactive glass affected the dissolution of unreacted particles most in the pH range typical for the extracellular fluid, *i.e.*, around 7.4. In contrast, the dissolution products had a minor impact on the glass dissolution in alkaline and acidic environments.

5. Conclusions

This work explored the impact of dissolution products in the immersion solution on the ion release from bioactive glass S53P4 in static alkaline (pH 9), physiological (pH 7.4) and acidic (pH 5) solutions. The as-prepared solutions initially contained no dissolved ions from the glass, while the solutions extracted after 24 and 72 h of immersion served as solutions with released ions in typical ratios dissolving from the glass. Glass particles immersed in the alkaline solution dissolved slowly and almost congruently, without forming typical reaction layers on the particle surfaces. The extracts slightly decreased ion release, but the reaction mechanisms were unchanged. Incongruent dissolution followed by the formation of typical silica-rich and calcium phosphate layers at the particle surfaces took place in the solution buffered at pH 7.4. The presence of dissolution products retarded the dissolution. Also, increasing calcium and phosphorus concentrations were identified in the silica-rich layer formed during immersion in the extracts. Finally, the dissolution was highly incongruent in the acidic solutions and increased almost linearly with immersion time. The dissolution products in the solution had a minor effect on the reactions. Despite the ion release, the pH of the buffered solutions increased only to a limited degree. Thus, changes in glass dissolution were mainly attributed to the dissolved ions in the solution. The results imply that implanted bioactive glass particles experiencing different local solution compositions react nonuniformly at a physiological pH and more uniformly in lower and higher pH environments.

Declaration of Competing Interest

The authors declare that they have no known competing financial interests or personal relationships that could have appeared to influence the work reported in this paper.
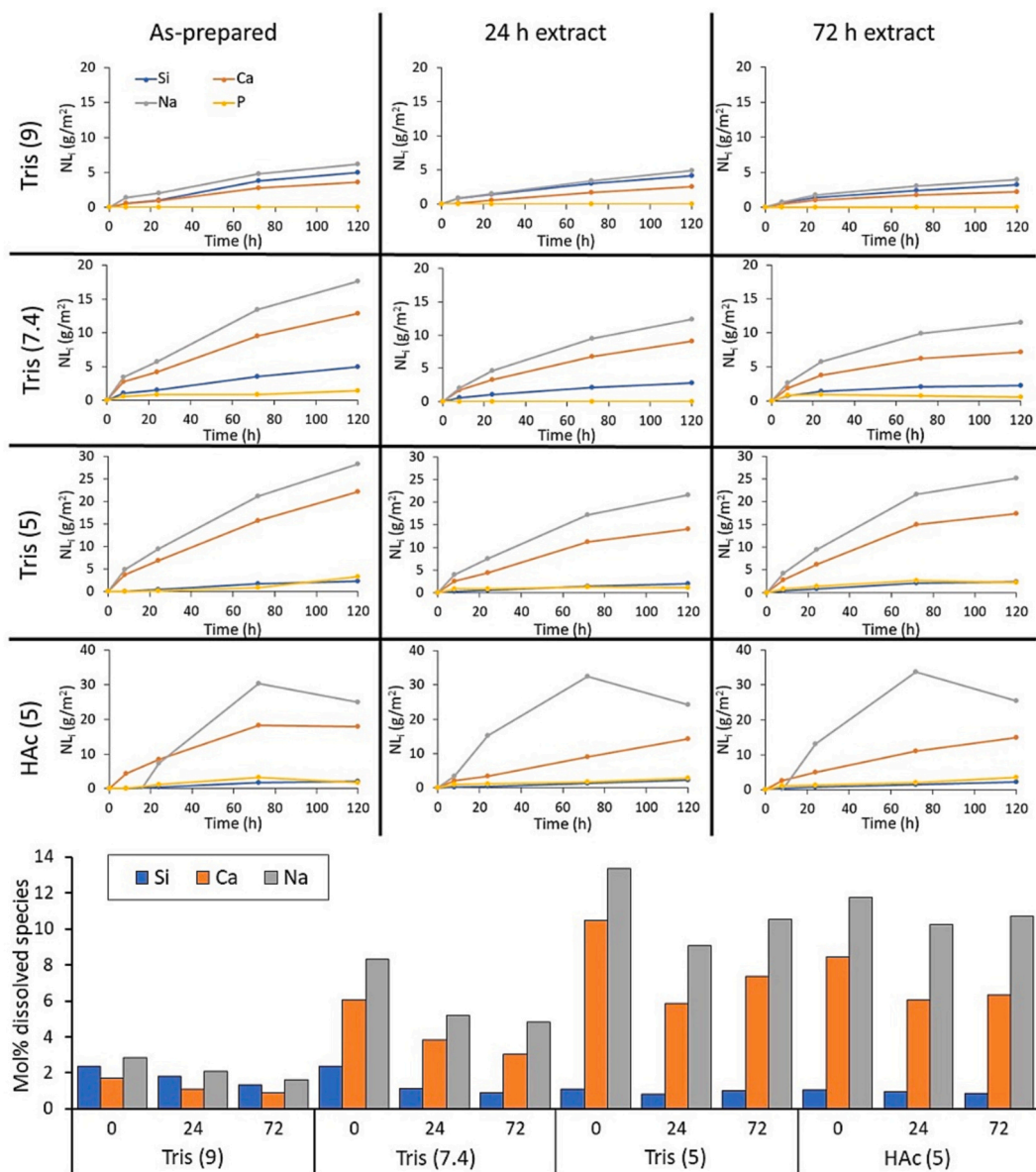
Fig. 6. Normalised mass loss rate from the unreacted S53P4 particles for 120 h of immersion and the dissolution of Si, Ca, and Na (mol%) at 120 h in the as-prepared solutions (0) and extracts (24 and 72).

Data availability

Data will be made available on request.

References

[1] D.J. Hulsen, N.A. van Gestel, J.A.P. Geurts, J.J. Arts, S53P4 bioactive glass, in: Management of Periprosthetic Joint Infections (PJIs), Elsevier, 2017, pp. 69–80, https://doi.org/10.1016/B978-0-08-100205-6.00004-5.
[2] M.N. Rahaman, D.E. Day, B.S. Bal, Q. Fu, S.B. Jung, L.F. Bonewald, et al., Bioactive glass in tissue engineering, Acta Biomater. 7 (2011) 2355–2373, https://doi.org/10.1016/j.actbio.2011.03.016.
[3] L.L. Hench, R.J. Splinter, W.C. Allen, T.K. Greenlee, Bonding mechanisms at the interface of ceramic prosthetic materials, J. Biomed. Mater. Res. 5 (1971) 117–141, https://doi.org/10.1002/jbm.820050611.
[4] Ö.H. Andersson, K. Vähätalo, A. Yli-Urpo, R.-P. Happonen, K.H. Karlsson, Short-Term Reaction Kinetics of Bioactive Glass in Simulated Body Fluid and in Subcutaneous Tissue. Bioceramics, Elsevier Ltd, 1994, pp. 67–72, https://doi.org/10.1016/B978-0-08-042144-5.50014-5.
[5] Ö.H. Andersson, I. Kangasniemi, Calcium phosphate formation at the surface of bioactive glass in vitro, J. Biomed. Mater. Res. 25 (1991) 1019–1030, https://doi.org/10.1002/jbm.820250808.
[6] E.J.G. Schepers, P. Ducheyne, L. Barbier, S. Schepers, Bioactive glass particles of narrow size range: a new material for the repair of bone defects, Implant. Dent. 2 (1993) 151–157, https://doi.org/10.1097/00008505-199309000-00002.
[7] L. Hench, The story of bioglass, J. Mater. Sci. Mater. Med. 17 (2006) 967–978, https://doi.org/10.1007/s10856-006-0432-z.
[8] L.L. Hench, Chronology of bioactive glass development and Clinical applications, NJGC 3 (2013) 67–73, https://doi.org/10.4236/njgc.2013.32011.
[9] L. Hupa, N.C. Lindfors, Bioactive Glass S53P4 – From a Statistically Suggested Composition to Clinical Success. Bioactive Glasses and Glass-Ceramics, John Wiley & Sons, Ltd, 2022, pp. 33–59, https://doi.org/10.1002/9781119724193.ch3.
[10] J.R. Jones, D.S. Brauer, L. Hupa, D.C. Greenspan, Bioglass and bioactive glasses and their impact on healthcare, Int. J. Appl. Glas. Sci. 7 (2016) 423–434, https://doi.org/10.1111/ijag.12252.
[11] N. Al Tamami, N. Bawazeer, M. Fieux, S. Zaouche, S. Tringali, Tolerance and safety of 45S5 bioactive glass used in obliteration procedures during middle ear surgery: preliminary results, Am. J. Otolaryngol. 41 (2020), 102542, https://doi.org/10.1016/j.amjoto.2020.102542.

[12] N.C. Lindfors, P. Hyvönen, M. Nyyssönen, M. Kirjavainen, J. Kankare, E. Gullichsen, et al., Bioactive glass S53P4 as bone graft substitute in treatment of osteomyelitis, Bone 47 (2010) 212–218, https://doi.org/10.1016/j.bone.2010.05.030.

[13] M. Gonzalez Moreno, M.E. Butini, E.M. Maiolo, L. Sessa, A. Trampuz, Antimicrobial activity of bioactive glass S53P4 against representative microorganisms causing osteomyelitis – real-time assessment by isothermal microcalorimetry, Colloids Surf. B: Biointerfaces 189 (2020), 110853, https://doi.org/10.1016/j.colsurfb.2020.110853.

[14] E. Munukka, O. Leppäranta, M. Korkeamäki, M. Vaahtio, T. Peltola, D. Zhang, et al., Bactericidal effects of bioactive glasses on clinically important aerobic bacteria, J. Mater. Sci. Mater. Med. 19 (2008) 27–32, https://doi.org/10.1007/s10856-007-3143-1.

[15] O. Leppäranta, M. Vaahtio, T. Peltola, D. Zhang, L. Hupa, M. Hupa, et al., Antibacterial effect of bioactive glasses on clinically important anaerobic bacteria in vitro, J. Mater. Sci. Mater. Med. 19 (2007), https://doi.org/10.1007/s10856-007-3018-5.

[16] L. Drago, D. Romanò, E. De Vecchi, C. Vassena, N. Logoluso, R. Mattina, et al., Bioactive glass BAG-S53P4 for the adjunctive treatment of chronic osteomyelitis of the long bones: an in vitro and prospective clinical study, BMC Infect. Dis. 13 (2013) 584, https://doi.org/10.1186/1471-2334-13-584.

[17] T.A.G. Van Vugt, J. Heidotting, J.J. Arts, J.J.W. Ploegmakers, P.C. Jutte, J.A. P. Geurts, Mid-term clinical results of chronic cavitary long bone osteomyelitis treatment using S53P4 bioactive glass: a multi-center study, J. Bone Joint. Infect. 6 (2021) 413–421, https://doi.org/10.5194/jbji-6-413-2021.

[18] L. Hupa, S. Fagerlund, J. Massera, L. Björkvik, Dissolution behavior of the bioactive glass S53P4 when sodium is replaced by potassium, and calcium with magnesium or strontium, J. Non-Cryst. Solids 432 (2016) 41–46, https://doi.org/10.1016/j.jnoncrysol.2015.03.026.

[19] L.L. Hench, Genetic design of bioactive glass, J. Eur. Ceram. Soc. 29 (2009) 1257–1265, https://doi.org/10.1016/j.jeurceramsoc.2008.08.002.

[20] J.R. Jones, Review of bioactive glass: from Hench to hybrids, Acta Biomater. 9 (2013) 4457–4486, https://doi.org/10.1016/j.actbio.2012.08.023.

[21] S. Fagerlund, P. Ek, L. Hupa, M. Hupa, Dissolution kinetics of a bioactive glass by continuous measurement, J. Am. Ceram. Soc. 95 (2012) 3130–3137, https://doi.org/10.1111/j.1551-2916.2012.05374.x.

[22] R.W. Douglas, T.M.M. El-Shamy, Reactions of glasses with aqueous solutions, J. Am. Ceram. Soc. 50 (1967) 1–8, https://doi.org/10.1111/j.1151-2916.1967.tb14960.x.

[23] L. Bingel, D. Groh, N. Karpukhina, D.S. Brauer, Influence of dissolution medium pH on ion release and apatite formation of bioglass 45S5, Mater. Lett. 143 (2015).

[24] R.K. Iler, The Solubility of Silica. The Chemistry of Silica, John Wiley & Sons, 1979, pp. 30–49.

[25] M.G. Cerruti, D. Greenspan, K. Powers, An analytical model for the dissolution of different particle size samples of bioglass ® in TRIS-buffered solution, Biomaterials 26 (2005) 4903–4911, https://doi.org/10.1016/j.biomaterials.2005.01.013.

[26] M. Siekkinen, O. Karlström, L. Hupa, Effect of local ion concentrations on the in vitro reactions of bioactive glass 45S5 particles, Int. J. Appl. Glas. Sci. 13 (2022) 695–707, https://doi.org/10.1111/ijag.16579.

[27] Constable P, Clinical Acid-Base Chemistry. Critical care nephrology, Elsevier, 2009, pp. 581–586, https://doi.org/10.1016/B978-1-4160-4252-5.50116-7.

[28] M. Cicuéndez, J.C. Doadrio, A. Hernández, M.T. Portolés, I. Izquierdo-Barba, M. Vallet-Regí, Multifunctional pH sensitive 3D scaffolds for treatment and prevention of bone infection, Acta Biomater. 65 (2018) 450–461, https://doi.org/10.1016/j.actbio.2017.11.009.

[29] L. Björkvik, X. Wang, L. Hupa, Dissolution of bioactive glasses in acidic solutions with the focus on lactic acid, Int. J. Appl. Glas. Sci. 7 (2016) 154–163, https://doi.org/10.1111/ijag.12198.

[30] C. Loke, J. Lee, S. Sander, L. Mei, M. Farella, Factors affecting intra-oral pH - a review, J. Oral Rehabil. 43 (2016) 778–785, https://doi.org/10.1111/joor.12429.

[31] D.S. Brauer, Bioactive glasses-structure and properties, Angew. Chem. Int. Ed. 54 (2015) 4160–4181, https://doi.org/10.1002/anie.201405310.

[32] A. Maçon, T. Kim, E. Valliant, K. Goetschius, R. Brow, D. Day, et al., A unified in vitro evaluation for apatite-forming ability of bioactive glasses and their variants, J. Mater. Sci. Mater. Med. 26 (2015) 1–10, https://doi.org/10.1007/s10856-015-5403-9.

[33] I.D. Xynos, A.J. Edgar, L.D.K. Buttery, L.L. Hench, J.M. Polak, Gene-expression profiling of human osteoblasts following treatment with the ionic products of bioglass® 45S5 dissolution, J. Biomed. Mater. Res. 55 (2001) 151–157, https://doi.org/10.1002/1097-4636(200105)55:2<151::AID-JBM1001>3.0.CO;2-D.

[34] M. Ojansivu, S. Vanhatupa, L. Björkvik, H. Häkkänen, M. Kellomäki, R. Autio, et al., Bioactive glass ions as strong enhancers of osteogenic differentiation in human adipose stem cells, Acta Biomater. 21 (2015) 190–203, https://doi.org/10.1016/j.actbio.2015.04.017.

[35] K. Vuornos, M. Ojansivu, J.T. Koivisto, H. Häkkänen, B. Belay, T. Montonen, et al., Bioactive glass ions induce efficient osteogenic differentiation of human adipose stem cells encapsulated in gellan gum and collagen type I hydrogels, Mater. Sci. Eng. C 99 (2019) 905–918, https://doi.org/10.1016/j.msec.2019.02.035.

[36] J.J.M. Damen, J.M. Ten Cate, Silica-induced precipitation of calcium phosphate in the presence of inhibitors of hydroxyapatite formation, J. Dent. Res. 71 (1992) 453–457, https://doi.org/10.1177/00220345920710030601.

[37] S. Maeno, Y. Niki, H. Matsumoto, H. Morioka, T. Yatabe, A. Funayama, et al., The effect of calcium ion concentration on osteoblast viability, proliferation and differentiation in monolayer and 3D culture, Biomaterials 26 (2005) 4847–4855, https://doi.org/10.1016/j.biomaterials.2005.01.006.

[38] M. Julien, S. Khoshniat, A. Lacreusette, M. Gatius, A. Bozec, E.F. Wagner, et al., Phosphate-dependent regulation of MGP in osteoblasts: role of ERK1/2 and Fra-1, J. Bone Miner. Res. 24 (2009) 1856–1868, https://doi.org/10.1359/jbmr.090508.

[39] M. Siekkinen, O. Karlström, L. Hupa, Dissolution of bioactive glass S53P4 in a three-reactor cascade in continuous flow conditions, Open Ceram. 13 (2023), 100327, https://doi.org/10.1016/j.oceram.2022.100327.

[40] P. Sepulveda, J.R. Jones, L.L. Hench, In vitro dissolution of melt-derived 45S5 and sol-gel derived 58S bioactive glasses, J. Biomed. Mater. Res. 6 (2002) 301–311, https://doi.org/10.1002/jbm.10207.

[41] G. Kirste, J. Brandt-Slowik, C. Bocker, M. Steinert, R. Geiss, D.S. Brauer, Effect of chloride ions in Tris buffer solution on bioactive glass apatite mineralization, Int. J. Appl. Glas. Sci. 8 (2017) 438–449, https://doi.org/10.1111/ijag.12288.

[42] N. Stone-Weiss, N.J. Smith, R.E. Youngman, E.M. Pierce, A. Goel, Dissolution kinetics of a sodium borosilicate glass in Tris buffer solutions: impact of Tris concentration and acid (HCl/HNO$_3$) identity, Phys. Chem. Chem. Phys. 23 (2021) 16165–16179, https://doi.org/10.1039/D0CP06425D.

[43] H.N. Po, N.M. Senozan, The Henderson-Hasselbalch equation: its history and limitations, J. Chem. Educ. 78 (2001) 1499, https://doi.org/10.1021/ed078p1499.

[44] D. Zhang, M. Hupa, H.T. Aro, L. Hupa, Influence of fluid circulation on in vitro reactivity of bioactive glass particles, Mater. Chem. Phys. 111 (2008) 497–502, https://doi.org/10.1016/j.matchemphys.2008.04.055.

[45] C.L. Trivelpiece, J.A. Rice, N.L. Clark, B. Kabius, C.M. Jantzen, C.G. Pantano, Corrosion of ISG fibers in alkaline solutions, J. Am. Ceram. Soc. 100 (2017) 4533–4547, https://doi.org/10.1111/jace.14950.

[46] Q. Qin, N. Stone-Weiss, T. Zhao, P. Mukherjee, J. Ren, J.C. Mauro, et al., Insights into the mechanism and kinetics of dissolution of aluminoborosilicate glasses in acidic media: impact of high ionic field strength cations, Acta Mater. 242 (2023), 118468, https://doi.org/10.1016/j.actamat.2022.118468.

[47] T. Kokubo, H. Takadama, How useful is SBF in predicting in vivo bone bioactivity? Biomaterials 27 (2006) 2907–2915, https://doi.org/10.1016/j.biomaterials.2006.01.017.

[48] M. Bohner, J. Lemaitre, Can bioactivity be tested in vitro with SBF solution? Biomaterials 30 (2009) 2175–2179, https://doi.org/10.1016/j.biomaterials.2009.01.008.

[49] J.R. Jones, P. Sepulveda, L.L. Hench, Dose-dependent behavior of bioactive glass dissolution, J. Biomed. Mater. Res. 58 (2001) 720–726, https://doi.org/10.1002/jbm.10053.

[50] A. Al-Noaman, S.C.F. Rawlinson, R.G. Hill, The role of MgO on thermal properties, structure and bioactivity of bioactive glass coating for dental implants, J. Non-Cryst. Solids 358 (2012) 3019–3027, https://doi.org/10.1016/j.jnoncrysol.2012.07.039.

[51] D. Zhang, M. Hupa, L. Hupa, In situ pH within particle beds of bioactive glasses, Acta Biomater. 4 (2008) 1498–1505, https://doi.org/10.1016/j.actbio.2008.04.007.

[52] S. Gin, P. Jollivet, M. Fournier, C. Berthon, Z. Wang, A. Mitroshkov, et al., The fate of silicon during glass corrosion under alkaline conditions: a mechanistic and kinetic study with the international simple glass, GCA 151 (2015) 68–85, https://doi.org/10.1016/j.gca.2014.12.009.

[53] N. Stone-Weiss, R.E. Youngman, R. Thorpe, N.J. Smith, E.M. Pierce, A. Goel, An insight into the corrosion of alkali aluminoborosilicate glasses in acidic environments, Phys. Chem. Chem. Phys. 22 (2020) 1881–1896, https://doi.org/10.1039/C9CP06064B.

[54] L. Varila, S. Fagerlund, T. Lehtonen, J. Tuominen, L. Hupa, Surface reactions of bioactive glasses in buffered solutions, J. Eur. Ceram. Soc. 32 (2012) 2757–2763, https://doi.org/10.1016/j.jeurceramsoc.2012.01.025.

[55] V. Cannillo, F. Pierli, I. Ronchetti, C. Siligardi, D. Zaffe, Chemical durability and microstructural analysis of glasses soaked in water and in biological fluids, Ceram. Int. 35 (2009) 2853–2869, https://doi.org/10.1016/j.ceramint.2009.03.029.